

Electronic structure of LaMnO₃ in the *ab initio* crystal Hartree-Fock approximation

Y.-S. Su, T. A. Kaplan, and S. D. Mahanti

Department of Physics and Astronomy, Center for Fundamental Materials Research, Michigan State University, East Lansing, Michigan 48824-1116

J. F. Harrison

Department of Chemistry, Center for Fundamental Materials Research, Michigan State University, East Lansing, Michigan 48824-1116
(Received 10 June 1999)

We find that an *ab initio* electronic structure calculation in the Hartree-Fock approximation (HFA) leads to the experimentally observed magnetic and orbital orderings in LaMnO₃, as well as its insulating character. While such agreement was also found in density-functional theories (DFT's), there are large differences in other physical predictions. The HFA results are discussed *vis a vis* two different DFT's and an embedded cluster theory, as well as x-ray photoemission and inelastic neutron scattering experiments.

I. INTRODUCTION

The divalent-metal doped rare-earth manganites have received a great deal of attention in recent years largely due to the colossal magnetoresistance (CMR) in these compounds. The phase diagrams of these manganites are very rich; the magnetic and conducting properties, as well as crystallographic structure, can vary substantially with temperature and doping concentration.¹ These properties alone, aside from the CMR, constitute an interesting research area. La_{1-x}Ca_xMnO₃ is a typical family of these manganites, with the CMR occurring in the region near $x = \frac{1}{3}$.¹ Here we focus on LaMnO₃ (the $x=0$ end member of the above family). Its properties, which involve magnetic and orbital ordering plus strong Jahn-Teller distortion, are interesting in their own right.

There has been a great deal of work on LaMnO₃; the papers most directly relevant here are Refs. 2–7. Saitoh *et al.*² obtained experimental photoemission results and interpreted them through a cluster configuration-interaction model. Local spin density approximation (LSDA) band calculations were reported in Refs. 3–5. In all three of the band calculations, the experimentally observed ground state magnetic ordering was found. The observed orbital ordering was obtained by Satpathy *et al.*⁴ (this property was not discussed in Refs. 3 and 5). The spin Hamiltonian, which governs the magnetic properties including the low-lying excitations (spin waves or magnons), was calculated by Solov'yev *et al.*⁶ within the LSDA. Hirota *et al.*⁷ determined the magnon dispersion via inelastic neutron scattering measurements, and claimed it to be consistent with the theory of Ref. 6. Sarma *et al.*³ found their LSDA density of states and calculated photoemission intensity to agree with the measurements of Saitoh *et al.*²

These facts would seem to have the theory of these properties of LaMnO₃ in satisfactory shape. However, the theories of Refs. 2 and 3, both of which apparently explain the photoemission data, disagree with each other. In Ref. 3 (in agreement with the other LSDA calculations of Refs. 4 and 5), the Mn *d* band lies near the top of the valence band, with the O *p* band lower than the *d* band, while in Ref. 2 the

opposite order occurs. Furthermore, an LDA+U band calculation gave the Mn *d* band below the O *p* band.⁴ Thus there are major differences between existing pictures, and they are of considerable importance, e.g., at stake is the nature of the band gap, O-*p*→Mn-*d* or Mn-*d*→Mn-*d* (the two possibilities have been called charge-transfer insulators or Mott-Hubbard insulators, respectively.⁸) We were thereby motivated to carry out calculations on LaMnO₃ using the Hartree-Fock approximation (HFA). HFA is a well-established theoretical approach, independent of the above methods, and thus can provide valuable comparison with the other results. Also, it is known that for some 3*d*-transition-metal oxides with perovskite-based structure, e.g., lanthanum cuprate and nickelate, LSDA failed⁹ and the HFA succeeded¹⁰ to predict correctly the ground state insulating property and the magnetic ordering.

Our HFA results show some surprising physical effects, and significant differences from LSDA. The correct magnetic and orbital orderings and insulating character are found in both theories. However, we find major differences in the occupied densities of states (e.g., the O *p* bands lie close to the top of the valence band in the HFA, more similar to the interpretation of Ref. 2 and the LDA+U results of Ref. 4). There is also a major difference in the effective spin Hamiltonians; yet the magnon dispersion curves of both theories are consistent with the neutron scattering experiment,⁷ as we will explain. Also, in apparent contrast to LSDA,^{4,11} a large spinless charge backflow, O⁻²2*p*→Mn⁺³3*d*, is found in HFA. Finally, the fundamental type of insulator differs in the two approximations: LSDA gives a band insulator (the gap doesn't exist for the cubic structure), HFA yields a Mott insulator (the gap exists for both the cubic and distorted structures).

II. METHOD

To our knowledge, ours is the first *ab initio* HFA calculation for this material.¹² The calculation makes use of the program CRYSTAL95.¹³ In LaMnO₃, the MnO₆ octahedra (denoted as [MnO₆]) are strongly Jahn-Teller distorted and rotated from the crystal axes by an appreciable amount, result-

TABLE I. HFA and LSDA (Ref. 5) energies of LaMnO₃ with various magnetic orderings. The energies shown are relative to the FM state of the cubic structure, in meV/Mn. (ins=insulator, met=metal.) The HFA energies are for the states with the observed orbital ordering (see text).

		FM	AAF	GAF	CAF	FI
HFA	cubic	0, ins	0.4, ins	34, ins	32, ins	16, ins
	orth	-1053, ins	-1055, ins	-1041, ins	-1039, ins	-1047, ins
LSDA	cubic	0, met	110, met	365, met		
	orth		-156, ins			

ing in an orthorhombic crystal structure (space group $Pnma$) with four symmetrically equivalent Mn per unit cell.¹⁴ We carried out the calculations on both the observed orthorhombic structure and a fictitious isovolume cubic structure in order to investigate the effect of the strong lattice distortion. The basis sets of Mn and O are those optimized for CaMnO₃.¹⁵ La is treated as a bare La⁺³ ion and represented by an effective core potential;¹⁶ a test of this approximation as well as other accuracy control parameters of the program will be discussed in Sec. IV.

The unit cell of the orthorhombic structure is close to the $\sqrt{2} \times \sqrt{2} \times 2$ supercell of the undistorted cubic perovskite structure. The longest side of the unit cell is chosen as c axis¹⁷ and the MnO₂ planes perpendicular to it are called basal planes.

III. RESULTS

A. Magnetic properties

For the orthorhombic structure, it can be shown that there are five collinear magnetic orderings that maintain the size of the unit cell. They are ferromagnetic (FM), A -type, G -type, and C -type antiferromagnetic (AAF, GAF, and CAF), and ferrimagnetic (FI) orderings, defined as follows. AAF: the Mn spins are parallel in a basal plane and antiparallel from plane to plane. GAF: each nearest-neighbor (NN) pair of Mn are antiparallel. CAF: each NN pair of Mn are antiparallel in a basal plane and parallel along the c axis. FI: one of the four Mn in a unit cell is antiparallel to the other three. HFA results for these ordered states are listed in Table I, together with LSDA results⁵ for comparison. It is seen that HFA predicts the ground state of LaMnO₃ to be an AAF insulator, in agreement with experiment.¹⁸ LSDA also makes the same prediction. In the cubic structure, both theories predict the FM state to have the lowest energy. However, there are substantial differences between the theories. For example, in HFA all states are insulating (for both cubic and orthorhombic structures), while in LSDA all states of the cubic structure are metallic.⁵ The band gaps (not shown in the table) in HFA are much larger than those in LSDA. From the results in the AAF column, it is seen that the crystal distortion lowers the energy per Mn by ~ 1 eV in HFA, vs 0.27 eV in LSDA. For the cubic case, it is seen that LSDA predicts much larger energy differences among the various magnetically ordered states.

The HFA energies of the five magnetically ordered states for the orthorhombic structure are used to map to an effective spin Hamiltonian (see Refs. 10 and 15 for discussion of the mapping). We add four-spin terms to the usual two-spin terms in the spin Hamiltonian¹⁹

$$H = \text{const} + \sum_{(i,j)} J_{ij} \vec{S}_i \cdot \vec{S}_j + \sum_{(i,j,k,l)} J_{ijkl} \times (\text{four-spin terms}) + \dots; \quad (1)$$

\vec{S}_i is the spin at (Mn) site i , J_{ij} and J_{ijkl} are exchange parameters, and each combination of summation indices is summed once. Since there are five energies, the mapping can determine four J 's plus the constant in H . We choose the J 's in the following way. We consider the one-band Hubbard model with NN intrabasal- and interbasal-plane hopping t_1, t_2 . Perturbation theory with the t_i small implies the spin Hamiltonian of Eq. (1). Keeping through fourth order terms, more than four J 's occur; however, only a particular subset of four can be determined by the five ordered states considered. This is the chosen set and is as follows: the intraplane NN J_1 , the interplane NN J_2 , the interplane next NN J_3 , and the interplane four-spin J_4 . Due to the distortion of the crystal structure, there are actually two types of J_3 and J_4 , denoted as $J_3^{(1)}$ and $J_3^{(2)}$,⁶ and $J_4^{(1)}$ and $J_4^{(2)}$. In the mapping here, only the average values of the two types of J 's are determined: J_3 is the average of $J_3^{(1)}$ and $J_3^{(2)}$, and similarly for J_4 . Note that the same mapping can also be done for the cubic case. This is possible because the existing orbital ordering (discussed later on) breaks the cubic symmetry and make, for example, J_1 not equal to J_2 .

The results of the mapping are listed in Table II. In both the cubic and orthorhombic cases, J_3 and J_4 are negligible. This supports the neglect of further neighbor terms, expected *a priori* to be small. The signs of J_1 and J_2 reflect the ground state magnetic properties (FM for the cubic and AAF for the orthorhombic). LSDA calculations by Solovyev *et al.* for the orthorhombic case give a qualitatively different picture.⁶ As shown in Table III, LSDA gives a much bigger J_3 ; also J_1 and J_2 are both ferromagnetic and they alone would yield a wrong magnetic state. It is the J_3 that turns the ground state from FM to AAF in the LSDA.

The spin wave spectrum of the system has been measured in a recent inelastic neutron scattering experiment and was fitted very well using a $2-J$ (J_1 and J_2) spin Hamiltonian by Hirota *et al.*⁷ The results are also included in Table III for

TABLE II. HFA J 's in the effective spin Hamiltonian of LaMnO₃, in meV.

	J_1	J_2	J_3	J_4
cubic	-2.1	-0.13	0.019	0.0049
orth.	-0.88	0.21	0.0036	0.00051

TABLE III. Comparison of the HFA, LSDA (Ref. 6), and experimental (Ref. 7) J 's in the spin Hamiltonian of LaMnO_3 , in meV.

	J_1	J_2	J_3
Exp	-1.67	1.21	~ 0
HFA	-0.88	0.21	~ 0
LSDA	-2.28	-0.78	0.78

comparison. Our HFA results are smaller in magnitude than the experimental values by about a factor of 2 for J_1 and 6 for J_2 . At first glance one would say that the experiment shows a 2- J character of the system and thus favors the HFA picture. However, as we analyze further, we find that this conclusion is not solid enough yet. Hirota *et al.* state that their experimental results are consistent with those of Solovyev *et al.* in the following sense. If one maps the 3- J model by Solovyev *et al.* to the following effective 2- J model:

$$\begin{cases} J_1^{(2J)} = J_1^{(3J)} \\ J_2^{(2J)} = J_2^{(3J)} + 4J_3^{(3J)} \end{cases} \quad (2)$$

(the factor of 4 in the second equality comes from the coordination number involved with J_3), then $J_1^{(2J)}$ and $J_2^{(2J)}$ have the right signs and are both about a factor of 2 too large in magnitude compared with the experimental values. By Eq. (2), the 3- J model and its effective 2- J model have identical spin wave dispersion along the c axis. Dispersion along several other directions is shown in Fig. 1. It is seen that the spin wave spectra of the two models are quite close. The difference is estimated to be about the size of the error bars of the experimental data cited. So at this point, the LSDA picture is not definitely ruled out. The issue could be settled by somewhat more accurate measurements.

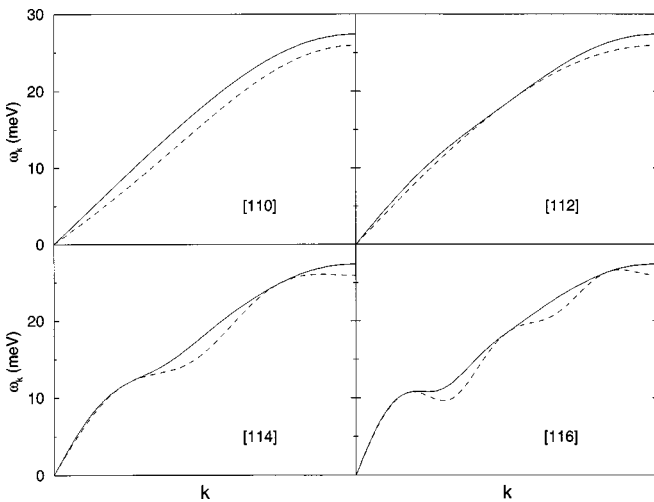


FIG. 1. The spin wave dispersions of the 3- J (solid line) and its effective 2- J (dashed) spin Hamiltonians, along four arbitrarily chosen directions. The values of J 's are those given by Solovyev *et al.* (Ref. 6). The k indexing follows the convention used in Ref. 7.

B. Spinless charge backflow and density of states

To our surprise, Mulliken population analysis (MPA) on the HFA results gives charges that deviate substantially from the formal valence picture, although the spin values do not show such deviation. We find $\text{Mn}^{+2.2}$, $\text{O}_I^{-1.7}$, and $\text{O}_{II}^{-1.75}$, while the Mn spin is 1.98; the formal valence picture is Mn^{+3} , O^{-2} , with Mn spin of 2. (O_I is the apical oxygen and O_{II} , the basal-plane oxygen.) We note that, due to the bare core approximation for La, these MPA results should only serve as an indication of deviation from the formal valence picture, not taken as being very accurate. A similar but more severe departure from the formal valence picture has been reported for an all-electron HFA calculation on CaMnO_3 ,¹⁵ where Mn was found to be $\text{Mn}^{+2.17}$ with spin $\frac{3.25}{2}$, compared with the nominal value Mn^{+4} with spin $\frac{3}{2}$. That is, there is a large nearly spinless backflow of electrons from O^{-2} to Mn^{+3} or Mn^{+4} . Such large changes in ionic charges would have obviously important consequences, e.g., on Madelung energies, phonon spectra, dielectric constant. How they would affect current simplified models is obscure, but certainly their implications for such models would have to be considered.

It must be pointed out that the MPA is basis set dependent, and can be very misleading when in the basis set there are diffuse basis functions that are appreciably occupied.^{20,21} However, the following considerations suggest that the deviation from the formal valence picture found here cannot be explained solely by basis set dependence. (i) We repeated the calculation with the most diffuse Mn d and O sp basis functions omitted from the basis set. This gave a very small change in the MPA, the result actually being further from the formal valence picture. (ii) The way that the MPA attributes an overlap charge to the two atoms involved is somewhat artificial and therefore results in an inherent uncertainty in the meaning of the MPA results. Moreover, when the MPA gives ridiculous results due to the presence of very diffuse basis functions in the basis set,^{20,21} there usually are large overlap charges. So smallness of the overlap charges is an indication of the reliability of the MPA results. In the present case, the overlap charges totally account for 0.06 electrons for Mn, considerably smaller than the deviation of the MPA charge of Mn from the formal charge. (iii) In contrast to MPA, the charge from the actual integration of the charge density over a reasonable volume (*vide infra*) around an atom is much more basis-set insensitive, and gives a realistic value of the HFA result (assuming a good basis set, of course). So this integration is a good check for verifying the correctness of MPA results. We did not do the integration for LaMnO_3 since the precise numbers will not be useful due to the bare core approximation for the La, as mentioned in the previous paragraph. Instead, we redid the all-electron calculation of Ref. 15 for CaMnO_3 , and then integrated the charge density over a cube around a Mn. The faces of the cube are perpendicular to the Mn-O bonds and pass through the minima of the charge density along the bonds, which gives the cube edge to be 1.8 Å (the cube is close in size to the Mn sphere of diameter 2.12 Å used in Ref. 5). The integrated charge for Mn was +2.52, close to the MPA result of +2.17. Further discussion of the La bare core approximation is given in Sec. IV, where it is suggested that a large deviation

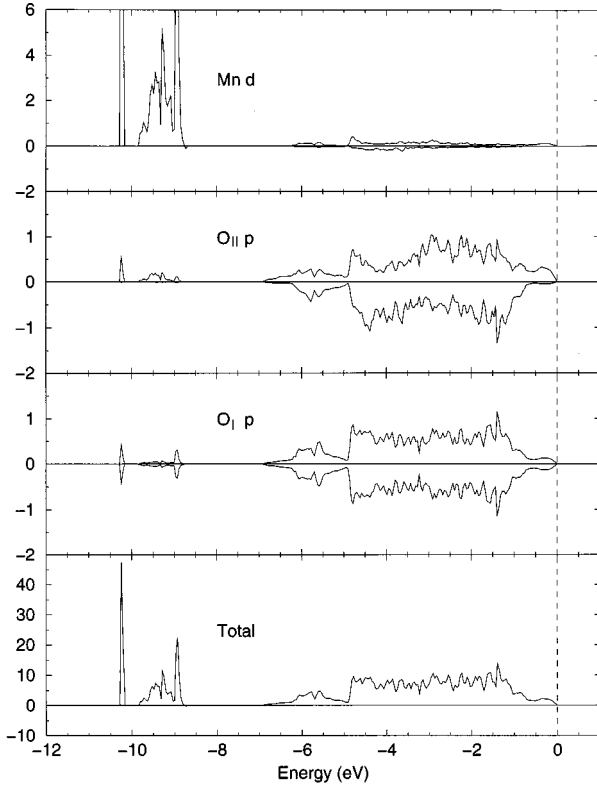


FIG. 2. The (projected) DOS of LaMnO_3 , with AAF ordering. Positive and negative DOS are for up- and down-spin states, respectively. Energies are relative to the top of the valence band. The projected Mn- d and $\text{O}_{||}p$ DOS are for Mn and O on an up-spin basal plane. The projected $\text{O}_{\perp}p$ and total DOS are symmetric for up- and down-spin. The down-spin part of the total DOS is omitted from the figure.

from formal valence, as found above, probably will hold true in more accurate HFA calculations.

The projected density of occupied states of LaMnO_3 is shown in Fig. 2. It is seen that a small amount of Mn- d projected density of states (DOS), both up and down, exists in the range of 0 to 6.9 eV below the top of the valence bands E_v , coinciding with the range of the $\text{O}p$ bands and accounting for the nearly spinless backflow. The large peaks (spin up) in the Mn- d projected DOS in the 8.7–10.3 eV range below E_v are associated with the Mn d bands, which are spin polarized and give the moment of Mn close to that predicted by the formal valence picture.

This HFA picture is rather different from previous LSDA calculations. First, to our knowledge, no departure from the formal valence picture has been reported in LSDA studies of the system. In fact, Satpathy *et al.*⁴ state that the charge states are close to nominal in their LSDA results. Second, the $\text{O}p$ bands lie above the Mn d bands in HFA, opposite to what LSDA predicts.^{3–5,11} The disagreement between HFA and LSDA in the order of $\text{O}p$ and transition metal d bands has also been seen for other systems.^{9,10,5,15}

We also note that LDA+U calculations⁴ show ordering of the $\text{O}p$ and Mn d bands very similar to our HFA results. Those calculations were disparaged⁵ on the grounds that the Mn spin turned out to be larger than the nominal value ($\frac{3}{2}$ for CaMnO_3). However, as far as we are aware, there is no theorem that the Mn spin must not be greater than nominal. In

fact intra-atomic exchange would tend to increase the Mn spin by polarizing electron transfer from O; also, we find in HFA an increase in Mn spin (as determined by integration of the spin density within a suitable cube centered at the Mn) over the nominal value for CaMnO_3 .

The HFA predictions of the charges on ions and the characters of the valence bands are consistent with the interpretation of a recent experiment by Saitoh *et al.*, who studied $\text{La}_{1-x}\text{Sr}_x\text{MnO}_3$ by photoemission and x-ray-absorption spectroscopy.² These authors determined that the character of the band gap of LaMnO_3 is of the p -to- d charge-transfer type while that of SrMnO_3 (corresponding to CaMnO_3 in our discussion) has considerable p - p character as well as p - d character. The HFA results (via the MPA) show that for LaMnO_3 and CaMnO_3 , the Mn- d electron population is roughly equal, while the $\text{O}p$ population gets reduced for the latter. This implies that the valence bands of CaMnO_3 consist of a smaller amount of $\text{O}p$ character than LaMnO_3 , which in turn suggests that there is a larger amount of $\text{O}p$ character in the conduction bands of CaMnO_3 . Combining this with the other HFA prediction that the $\text{O}p$ bands are the highest occupied bands can explain the above experimental observation. Saitoh *et al.* also reported that the Mn- d electron population is 4.5 for LaMnO_3 and 3.8 for SrMnO_3 , a considerable deviation from the formal valence picture similar to (although not as severe as) that predicted by the HFA, which we find to be about 4.7 for both LaMnO_3 and CaMnO_3 . The most surprising aspect of the Saitoh *et al.* work² is that their calculation showed a large reduction in photoemission intensity of the Mn d band as compared to the density of states (due to matrix-element effects). We intend to calculate that intensity using our HFA wave functions to check this.

C. Orbital ordering

We now discuss orbital ordering—this is ordering of the single e_g orbital occupied at each Mn. In the observed structure, each $[\text{MnO}_6]$ is stretched substantially along one axis and is rotated by 10° – 15° from its orientation in the cubic structure. Disregarding the rotation for simplicity, the stretched axes lie in the basal plane, alternating in direction by 90° , and this pattern repeats along the c axis. The stretching, being driven by the Jahn-Teller splitting of the e_g states, leads to an expected orbital ordering—the single occupied e_g orbital at each Mn is $d(3z^2 - r^2)$ type with its axial symmetry along the stretched axis of the associated $[\text{MnO}_6]$. This orbital ordering is indeed found in our HFA solutions, by plotting the spin density. A combination of the three t_{2g} and one e_g electrons (nominally the only unpaired electrons in the system) dictates a unique shape in the spin density distribution, which therefore can be used to identify which e_g orbital is actually occupied. For example, Fig. 3 shows the spin density at a Mn with the $d(3x^2 - r^2)$ orbital occupied (the z direction is along the c axis). This orbital ordering, which was predicted long ago by Goodenough,²² has also been obtained in LSDA calculations,⁴ and was recently confirmed in experiments.²³

In our study, we obtain the same orbital ordering for all trials with various magnetic orderings as well as initial conditions used to start the Hartree-Fock calculations, for the observed orthorhombic structure. However, for the cubic

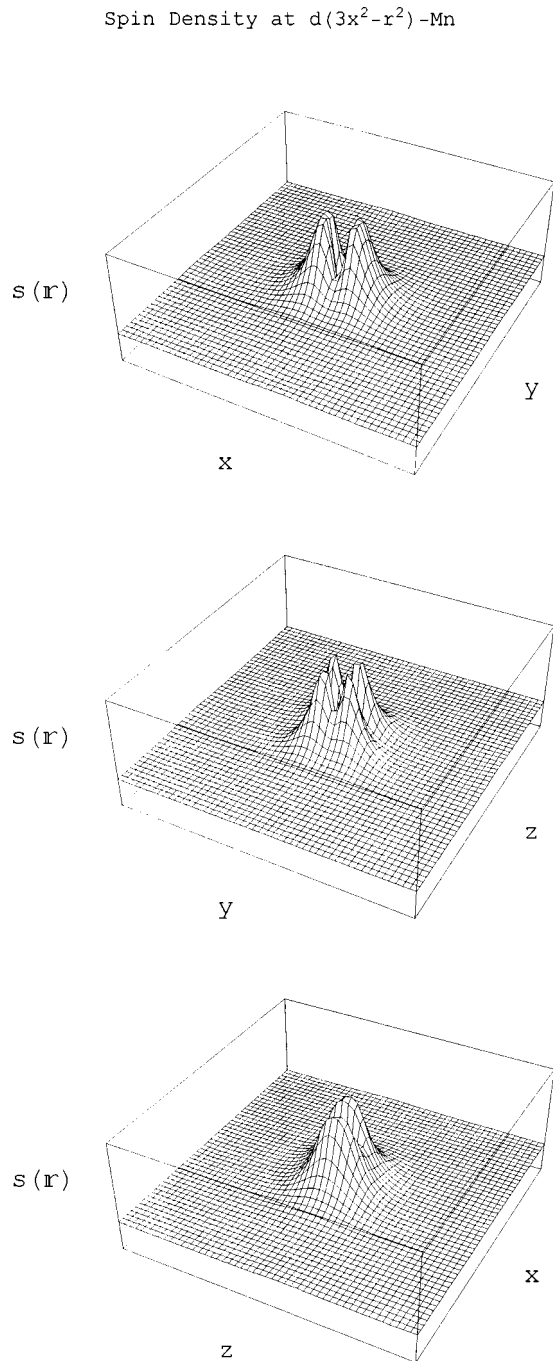


FIG. 3. The spin density on the xy , yz , and zx planes at a Mn with the $d(3x^2-r^2)$ and three t_{2g} orbitals occupied. The plotting region is about $(3.9 \text{ \AA})^2$, centered at the Mn. The slightly off of the symmetry axes of the distribution from the x , y , and z axes is a result of the rotations of the $[\text{MnO}_6]$ in the observed crystal structure.

structure we find a variety of orbital orderings by starting with different initial conditions. This is probably due to the absence of the Jahn-Teller distortion which would stabilize the occupancy pattern of the e_g orbitals.²⁴ Table IV lists the energies of the various states we have obtained in the cubic case. Roughly speaking, the results suggest that the energy scales associated with the change in crystal structure (cubic to orthorhombic), orbital ordering (in the cubic structure), and magnetic ordering are in the ranges of 1, 0.1, and 0.01 eV/Mn, respectively.

TABLE IV. HFA energies of different magnetic and orbital ordering states for the cubic structure. The symbol $d(3z^2-r^2)$ means that the e_g electron is of this type for all Mn, similarly for $d(x^2-y^2)$. The third one, $d(3x^2-r^2)/d(3y^2-r^2)$, is the observed ordering of the orthorhombic structure, as discussed in the text. Energies are relative to the AAF state of the orthorhombic structure, in meV/Mn.

	FM	AAF	GAF	CAF
$d(3z^2-r^2)$		1147.4		
$d(x^2-y^2)$		1165.9	1145.0	1157.5
$d(3x^2-r^2)/d(3y^2-r^2)$	1054.8	1055.2	1088.9	1087.2

IV. DISCUSSION AND SUMMARY

The extreme smallness of the various energy differences between magnetic states requires a discussion of the numerical accuracy of our calculations. The sources of error are¹³ the tolerance in the direct-space summations of Coulomb and exchange series (controlled in the program by five parameters called TOLINTEG), the number of sampling points for the Brillouin zone integration (controlled by a shrinking factor IS), and the finite basis sets used. The presented results of this work were calculated using TOLINTEG of (7, 7, 7, 7, 14) and IS of 6. IS=6 translates to 80 asymmetric k points in the Brillouin zone and is more than adequate for our need of accuracy; the total energy obtained from using IS=4 (30 asymmetric k points) deviated by less than 0.003 meV/Mn. The deviation of total energy due to change of TOLINTEG is much larger; by using (8, 8, 8, 8, 16) for TOLINTEG, we observed that the total energy changed by about 50 meV/Mn. However, the energy differences between various magnetic states in the test remained quite stable, typically only varying by ~ 0.1 meV/Mn. Concerning the errors due to the finite basis sets, we expect the most severe should come from the La bare core approximation, which we now discuss.

The test of the bare La^{+3} ion approximation consisted of adding to the La^{+3} core an optimized d shell consisting of a single primitive Gaussian (0.32 Bohr^{-2} is the optimized exponent). The total energy decreased by about 2 eV/Mn; however, the energy differences between the various magnetic states changed by only ~ 0.1 meV/Mn (a few %), and the change in the occupied band structure (not shown) is small. Similar behavior of the basis set dependence was also found in studies of other systems.¹⁰ The charges found in the test were $\text{La}^{+2.58}$, $\text{Mn}^{+2.14}$, $\text{O}_I^{-1.55}$, and $\text{O}_{II}^{-1.59}$. Interestingly, 0.42 electrons per La occupied the added La d shell, but these electrons were taken from oxygen, making the results even further from the formal valence picture.

To summarize, our HFA results on LaMnO_3 give a dramatically different picture from that of previous LSDA calculations, although for some properties, e.g., orbital and magnetic ordering, the two theories agree. This agreement is surprising in view of, but certainly not inconsistent with, the large differences. Some of the HFA predictions have been supported by experiment. In particular, the HFA spin Hamiltonian is consistent with a spin wave experiment, but the present accuracy of the experiment is not quite sufficient to distinguish conclusively between the HFA and LSDA results. The DOS in HFA is consistent with one interpretation² of a photoemission experiment.² However, it is not consis-

tent with another interpretation³ of the same experimental results, based on LSDA. Further, the DOS in LDA+U theory⁴ is more similar to the HFA result, and is definitely inconsistent with the LSDA result. We can conclude that our HFA results have added weight to the picture where the top of the valence band consists predominantly of O-*p* states, as found in the LDA+U (Ref. 4) and the cluster model inter-

pretation of photoemission results² (in contradiction to the LSDA results³⁻⁵).

ACKNOWLEDGMENTS

We thank R. Liu, A. Fujimori, D. Singh, Y. Tokura, and S. Billinge for useful discussions, and T. Egami for pointing out the paper of Saitoh *et al.* and encouragement.

-
- ¹S-W. Cheong and C. H. Chen, in *Colossal Magnetoresistance, Charge Ordering and Related Properties of Manganese Oxides*, edited by C. N. R. Rao and B. Raveau (World Scientific, Singapore, 1998).
- ²T. Saitoh, A. E. Boucquet, T. Mizokawa, H. Namatame, A. Fujimori, M. Abbate, Y. Takeda, and M. Takano, *Phys. Rev. B* **51**, 13 942 (1995).
- ³D. D. Sarma, N. Shanthi, S. R. Barman, N. Hamada, H. Sawada, and K. Terakura, *Phys. Rev. Lett.* **75**, 1126 (1995).
- ⁴S. Satpathy, Z. S. Popović, and F. R. Vukajlović, *Phys. Rev. Lett.* **76**, 960 (1996).
- ⁵W. E. Pickett and D. Singh, *Phys. Rev. B* **53**, 1146 (1996).
- ⁶I. Solovyev, N. Hamada, and K. Terakura, *Phys. Rev. Lett.* **76**, 4825 (1996).
- ⁷K. Hirota, N. Kaneko, A. Nishizawa, and Y. Endoh, *J. Phys. Soc. Jpn.* **65**, 3736 (1996).
- ⁸J. Zaanen, G. Sawatzky, and J. W. Allen, *Phys. Rev. Lett.* **55**, 418 (1985); **53**, 2339 (1984); J. Zaanen and G. Sawatzky, *J. Solid State Chem.* **88**, 8 (1990).
- ⁹W. E. Pickett, *Rev. Mod. Phys.* **61**, 433 (1996).
- ¹⁰Y-S. Su, T. A. Kaplan, S. D. Mahanti, and J. F. Harrison, *Phys. Rev. B* **59**, 10 521 (1999).
- ¹¹W. E. Pickett and D. J. Singh, in *Physics of Manganites*, edited by T. A. Kaplan and S. D. Mahanti (Kluwer Academic, New York, 1999), p. 87.
- ¹²There have been HFA calculations on *model* systems, e.g., T. Mizokawa and A. Fujimori, *Phys. Rev. B* **51**, 12 880 (1995).
- ¹³R. Dovesi, V. R. Saunders, C. Roetti, M. Causà, N. M. Harrison, R. Orlando, and E. Aprà, *CRYSTAL95 User's Manual* (University of Torino, Torino, 1996).
- ¹⁴J. B. A. Elemans, B. van Laar, K. R. van der Veen, and B. O. Loopstra, *J. Solid State Chem.* **3**, 238 (1971).
- ¹⁵F. F. Fava, Ph D'Arco, R. Orlando, and R. Dovesi, *J. Phys.: Condens. Matter* **9**, 489 (1997).
- ¹⁶P. J. Hay and W. R. Wadt, *J. Chem. Phys.* **82**, 270 (1985).
- ¹⁷In the *Pnma* space group defined in the *International Tables For X-Ray Crystallography*, Vol. I, edited by N. F. M. Henry and K. Lonsdale (The Kynoch Press, Birmingham, England), the longest side is along the *b* axis.
- ¹⁸G. H. Jonker and J. H. van Santen, *Physica (Amsterdam)* **16**, 337 (1950); J. H. van Santen and G. H. Jonker, *ibid.* **16**, 599 (1950); E. O. Wollan and W. C. Koehler, *Phys. Rev.* **100**, 545 (1955).
- ¹⁹M. Takahashi, *J. Phys. C* **10**, 1289 (1977).
- ²⁰T. A. Kaplan, H. Chang, S. D. Mahanti, and J. F. Harrison, in *Electronic Properties of Solids Using Cluster Methods*, edited by T. A. Kaplan and S. D. Mahanti (Plenum, New York, 1995), p. 73.
- ²¹P. S. Bagus, F. Illas, C. Sousa, and G. Pacchioni, in *Electronic Properties of Solids Using Cluster Methods* (Ref. 20), p. 93.
- ²²J. B. Goodenough, *Phys. Rev.* **100**, 564 (1955).
- ²³Y. Murakami, J. P. Hill, D. Gibbs, M. Blume, I. Koyama, M. Tanaka, H. Kawata, T. Arima, Y. Tokura, K. Hirota, and Y. Endoh, *Phys. Rev. Lett.* **81**, 582 (1998).
- ²⁴T. Mizokawa and A. Fujimori, see Ref. 12.